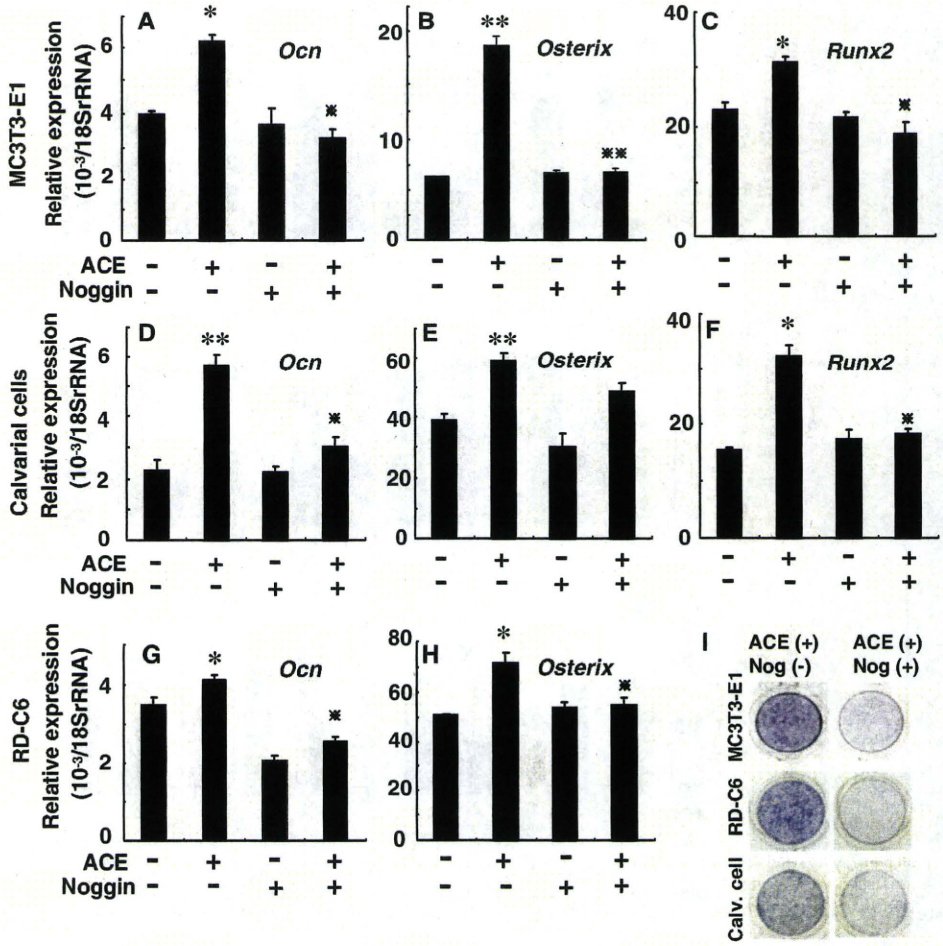

Fig. 3. Effects of ACE and noggin on *Osteocalcin* (*Ocn*), *Osterix* and *Runx2* mRNA expression in MC3T3-E1 cells (A, B, C), calvarial cells (D, E, F), and RD-C6 cells (G, H). The cells were cultured for 6 days in the presence or absence of ACE (30 μM) with or without noggin (500 ng/ml) treatment. Histochemical detection of ALP activity in MC3T3-E1 cells, RD-C6 cells and calvarial cells (I). All of the cells were treated with ACE (30 μM) for 6 days in the presence or absence of noggin (Nog), and ALP activity was detected as described in Section 2. $^{*}P < 0.05$, $^{**}P < 0.01$: significantly different from control culture [ACE (−), Noggin (−)], ※$P < 0.05$, ※※$P < 0.01$: significantly different from ACE treated cells [ACE (+), Noggin (−)].

cause ACE treatment also stimulated *Alp* and *Osteocalcin* mRNAs expression at doses over 5 μM in MC3T3-E1 cells on day 3 after the treatment, these effects may be closely related to increase in BMP levels due to ACE treatment. In contrast, the 3-day ACE treatment induced no apparent increases in the *Bmp-2*, *Bmp-4* and *Bmp-7* mRNA expression levels in RD-C6 cells, but the 6-day treatment significantly upregulated the *Bmp-2* and *Bmp-7* mRNA expression levels in this cell line. Interestingly, ACE failed to increase *Osteocalcin* mRNA expression on day 3 after ACE treatment, but was induced on day 9 after the treatment in RD-C6 cells (Fig. 1D). These results indicate that delayed induction of *Osteocalcin* mRNA expression in RD-C6 by ACE treatment may be related to the delayed increase in BMPs expression levels in response to ACE treatment in this cell line. In contrast, ACE stimulated *Alp* mRNA expression as early as on day 3 after the treatment in RD-C6 cells (Fig. 1C). This suggests that RD-C6 cells produced BMPs other than BMP-2, BMP-4, and BMP-7 in response to ACE or that a signaling pathway other than the BMP signaling is involved in this anabolic action. The Wnt/β-catenin signaling pathway is one such candidate because this signaling pathway plays a crucial role in osteoblast differentiation [31]. Whether Wnt/β-catenin signaling is involved in ACE-induced osteoblast differentiation is of considerable interest and is under investigation in our group. These studies will provide important information for identifying the target molecules of ACE in osteoblast differentiation.

The occurrence of osteoblast differentiation depends on the cell number in *in vitro* cell culture systems. Since ACE stimulated the proliferation of osteoblastic cells, we investigated whether the stimulatory effects of ACE on osteoblast differentiation occurred in MC3T3-E1 cells in the postconfluent state. The results of this experiment revealed that ACE stimulated osteoblast differentiation even after the postconfluent stage by increasing *Osteocalcin*, *Osterix*, and *Runx2* mRNA expression, although an early differentiation marker, *Alp* mRNA expression, was not stimulated. Interestingly, the induction of BMPs by ACE treatment was not apparent compared to that observed in proliferating-stage cultures of MC3T3-E1 cells (Fig. 4A–C). These results suggested that the stimulatory effects of ACE on osteoblast differentiation partly depend on the cell proliferation effect of ACE, and that ACE-induced BMP induction preferentially occurred at a cell proliferation stage.

In summary, this is the first study to show that a natural compound, ACE, isolated from *A. nikoense* Maxim exerts stimulatory effects on osteoblast differentiation through BMP action mediated by Runx2-dependent and Runx2-independent pathways. These results suggest that ACE is a candidate anabolic agent for stimulating bone formation. This effect of ACE treatment will be useful with re-

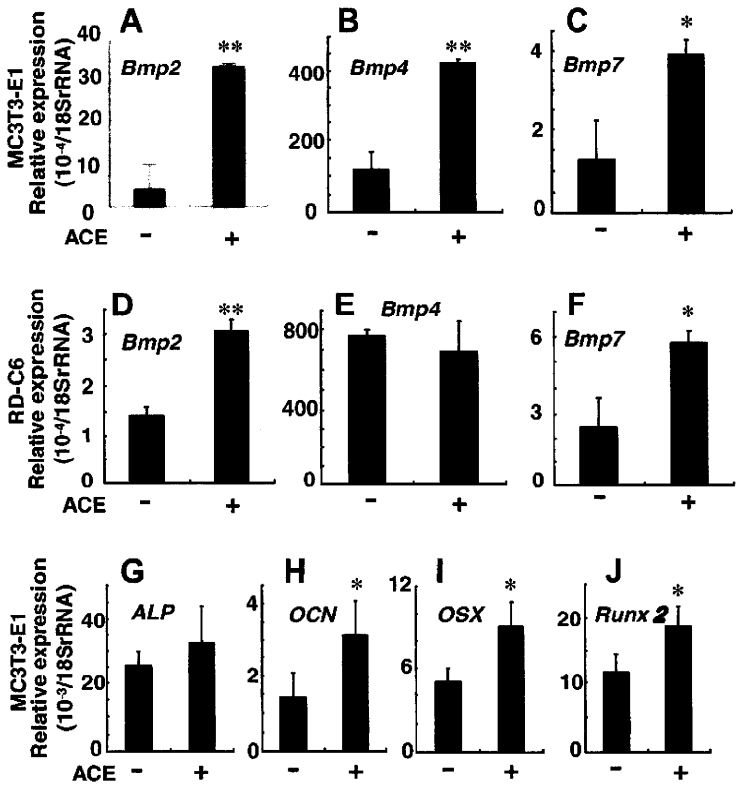

Fig. 4. A-F: Effects of ACE on *Bmp2*, *Bmp4* and *Bmp7* mRNA expression in MC3T3-E1 (A, B, C) and RD-C6 cells (D, E, F). MC3T3-E1 cells (A, B, C) were treated with ACE (30 μM) for 3 days, while RD-C6 cells (D, E, F) were treated for 6 days. G-J: Effects of ACE on *Alp*, *Osteocalcin* (*Ocn*), *Osterix*, and *Runx2* mRNA expression levels in MC3T3-E1 cells in the postconfluent state (G-I). ACE (30 μM) was added into the MC3T3-E1 cell culture on day 3 (confluent state), and mRNA expression was assessed after 3 days of the treatment. $^{*}P < 0.05$, $^{**}P < 0.01$.

gard to developing therapeutic agents for bone diseases such as bone repair and osteoporosis.

Acknowledgments

This work was supported by a Grant-in-Aid for Scientific Research from the Japan Society for the Promotion of Science (Nos. 22249061 and 21659420) and Health and Labour Sciences Research Grants from the Ministry of Health, Labour, and Welfare (No. 21040101) to A.Y., and by the Global Center of Excellence (GCOE) Program; International Research Center for Molecular Science in Tooth and Bone Diseases, Tokyo Medical and Dental University.

References

[1] J.M. Wozney, V. Rosen, A.J. Celeste, L.M. Mitsock, M.J. Whitters, R.W. Kriz, R.M. Hewick, E.A. Wang, Novel regulators of bone formation: molecular clones and activities, Science 242 (1988) 1528–1534.

[2] A. Yamaguchi, T. Komori, T. Suda, Regulation of osteoblast differentiation mediated by bone morphogenetic proteins, hedgehogs, and Cbfa1, Endocr. Rev. 21 (2000) 393–411.

[3] M.H. Lee, Y.J. Kim, H.J. Kim, H.D. Park, A.R. Kang, H.M. Kyung, J.H. Sung, J.M. Wozney, H.M. Ryoo, BMP-2-induced Runx2 expression is mediated by Dlx5, and TGF-beta 1 opposes the BMP-2-induced osteoblast differentiation by suppression of Dlx5 expression, J. Biol. Chem. 278 (2003) 34387–34394.

[4] T. Komori, H. Yagi, S. Nomura, A. Yamaguchi, K. Sasaki, K. Deguchi, Y. Shimizu, R.T. Bronson, Y.-H. Gao, M. Inada, M. Sato, R. Okamoto, Y. Kitamura, S. Yoshiki, T. Kishimoto, Targeted disruption of Cbfa1 results in a complete lack of bone formation owing to maturational arrest of osteoblasts, Cell 89 (1997) 755–764.

[5] F. Otto, A.P. Thornell, T. Crompton, A. Denzel, K.C. Gilmour, I.R. Rosewell, G.W. Stamp, R.S. Beddington, S. Mundlos, B.R. Olsen, P.B. Selby, M.J. Owen, Cbfa1, a candidate gene for cleidocranial dysplasia syndrome, is essential for osteoblast differentiation and bone development, Cell 89 (1997) 765–771.

[6] P. Ducy, R. Zhang, V. Geoffroy, A.L. Ridall, G. Karsenty, Osf2/Cbfa1: a transcriptional activator of osteoblast differentiation, Cell 89 (1997) 747–754.

[7] K. Nakashima, X. Zhou, G. Kunkel, Z. Zhang, J.M. Deng, R.R. Behringer, B. De Crombrugghe, The novel zinc finger-containing transcription factor osterix is required for osteoblast differentiation and bone formation, Cell 108 (2002) 17–29.

[8] M.R. Urist, Bone: formation by autoinduction, Science 150 (1965) 893–899.

[9] A. Yamaguchi, T. Katagiri, T. Ikeda, J.M. Wozney, V. Rosen, E.A. Wang, A.J. Kahn, T. Suda, S. oshiki, Recombinant human bone morphogenetic protein-2 stimulates osteoblastic maturation and inhibits myogenic differentiation in vitro, J. Cell Biol. 113 (1991) 681–687.

[10] T. Katagiri, A. Yamaguchi, K. Komaki, E. Abe, N. Takahashi, T. Ikeda, V. Rosen, J.M. Wozney, A. Fujisawa-Sehara, T. Suda, Bone morphogenetic protein-2 converts the differentiation pathway of C2C12 myoblasts into the osteoblast lineage, J. Cell Biol. 127 (1994) 1755–1766.

[11] A. Yamaguchi, T. Ishizuya, N. Kintou, Y. Wada, T. Katagiri, J.M. Wozney, V. Rosen, S. Yoshiki, Effects of BMP-2, BMP-4 and BMP-6 on osteoblast differentiation of bone marrow-derived stromal cell lines, ST2 and MC3T3-G2/PA6, Biochem. Biophys. Res. Commun. 220 (1996) 366–371.

[12] T.K. Sampath, J.C. Maliakal, P.V. Hauschka, W.K. Jones, H. Sasak, R.F. Tucker, K.H. White, J.E. Coughlin, M.M. Tucker, R.H.L. Pang, C. Corbett, E. Ozkaynak, H. Oppermann, D.C. Rueger, Recombinant human osteogenic protein-1 (hOP-1) induces new bone formation in vivo with a specific activity comparable with natural bovine osteogenic protein and stimulates osteoblast proliferation and differentiation in vitro, J. Biol. Chem. 267 (1992) 20352–20362.

[13] I.R. Garrett, Anabolic agents and the bone morphogenetic protein pathway, Curr. Top. Dev. Biol. 78 (2007) 127–171.

[14] A.P. White, A.R. Vaccaro, J.A. Hall, P.G. Whang, B.C. Friel, M.D. McKee, Clinical applications of BMP-7/OP-1 in fractures, nonunions and spinal fusion, Int. Orthop. 31 (2007) 735–741.

[15] H.A. Awad, X. Zhang, D.G. Reynolds, R.E. Guldberg, R.J. O'Keefe, E.M. Schwarz, Recent advances in gene delivery for structural bone allografts, Tissue Eng. 13 (2007) 1973–1985.

[16] P.C. Bessa, M. Casal, R.L. Reis, Bone morphogenetic proteins in tissue engineering: the road from laboratory to clinic, part II (BMP delivery), J. Tissue Eng. Regen. Med. 2 (2008) 81–96.

[17] K. Nakagawa, Y. Imai, Y. Ohta, K. Takaoka, Prostaglandin E2 EP4 agonist (ONO-4819) accelerates BMP-induced osteoblastic differentiation, Bone 41 (2007) 543–548.
[18] T. Namikawa, H. Terai, M. Hoshino, M. Kato, H. Toyoda, K. Yano, H. Nakamura, K. Takaoka, Enhancing effects of a prostaglandin EP4 receptor agonist on recombinant human bone morphogenetic protein-2 mediated spine fusion in a rabbit model, Spine 32 (2007) 2294–2299.
[19] G. Mundy, R. Garrett, S. Harris, J. Chan, D. Chen, G. Rossini, B. Boyce, M. Zhao, G. Gutierrez, Stimulation of bone formation in vitro and in rodents by statins, Science 286 (1999) 1946–1949.
[20] G. Luisetto, V. Camozzi, Statins, fracture risk, and bone remodeling, J. Endocrinol. Invest. 32 (2009) 32–37.
[21] H. Hojo, K. Igawa, S. Ohba, F. Yano, K. Nakajima, Y. Komiyama, T. Ikeda, A.C. Lichtler, J.T. Woo, T. Yonezawa, T. Takato, U.I. Chung, Development of high-throughput screening system for osteogenic drugs using a cell-based sensor, Biochem. Biophys. Res. Commun. 376 (2008) 375–379.
[22] M. Nagai, M. Kubo, M. Fujita, T. Inoue, M. Matsuo, Studies on the constituents of Aceraceae Plants. II. Structure of aceroside I, a glucose of a novel cyclic diarylheptanoids from *Acer nikoense* Maxim, Chem. Pharm. Bull. 26 (1978) 2805–2810.
[23] M. Nagai, M. Kubo, M. Fujita, T. Inoue, M. Matsuo, Acerogenin A, a novel cyclic diarylheptanoid, J. Chem. Soc. Chem. Commun. (1976) 338–339.
[24] T. Morikawa, J. Tao, K. Ueda, H. Matsuda, M. Yoshikawa, Medicinal foodstuffs. XXXI. Structures of new aromatic constituents and inhibitors of degranulation in RBL-2H3 cells from Japanese folk medicine, the stem bark of *Acer nikoense*, Chem. Pharm. Bull. 51 (2003) 62–67.
[25] M. Shinoda, S. Ohta, M. Kumasaka, M. Fujita, M. Nagai, T. Inoue, Protective effect of the bark of *Acer nikoense* on hepatic injury induced by carbon, Shoyakugaku Zasshi 40 (1986) 177–181.
[26] T. Morikawa, J. Tao, I. Toguchida, H. Matsuda, M. Yoshikawa, Structures of new cyclic diarylheptanoids and inhibitors of nitric oxide production from Japanese folk medicine *Acer nikoense*, J. Nat. Prod. 66 (2003) 86–91.
[27] H. Morita, J. Deguchi, Y. Motegi, S. Sato, C. Aoyama, J. Takeo, M. Shiro, Y. Hirasawa, Cyclic diarylheptanoids as Na^+-glucose cotransporter (SGLT) inhibitors from *Acer nikoense*, Bioorg. Med. Chem. Lett. 20 (2010) 1070–1074.
[28] T. Liu, Y. Gao, K. Sakamoto, T. Minamizato, K. Furukawa, T. Tsukazaki, Y. Shibata, K. Bessho, T. Komori, A. Yamaguchi, BMP-2 promotes differentiation of osteoblasts and chondroblasts in Runx2-deficient cell lines, J. Cell Physiol. 211 (2007) 728–735.
[29] C.G. Bellows, J.E. Aubin, J.N. Heersche, M.E. Antosz, Mineralized bone nodules formed in vitro from enzymatically released rat calvaria cell populations, Calcif. Tissue Int. 38 (1986) 143–154.
[30] V. Rosen, BMP and BMP inhibitors in bone, Ann. NY Acad. Sci. 1068 (2006) 19–25.
[31] R. Baron, G. Rawadi, S. Roman-Roman, Wnt signaling: a key regulator of bone mass, Curr. Top. Dev. Biol. 76 (2006) 103–127.

Histopathology 2011, **58**, 531–542. DOI: 10.1111/j.1365-2559.2011.03759.x

Down-regulation of keratin 4 and keratin 13 expression in oral squamous cell carcinoma and epithelial dysplasia: a clue for histopathogenesis

Kei Sakamoto,[1] Tadanobu Aragaki,[2] Kei-ichi Morita,[3] Hiroshi Kawachi,[4] Kou Kayamori,[1] Shoichi Nakanishi,[1] Ken Omura,[3] Yoshio Miki,[5,6] Norihiko Okada,[7] Ken-ichi Katsube,[1] Toichiro Takizawa[8] & Akira Yamaguchi[1]

Sections of [1]Oral Pathology, [2]Maxillofacial Surgery, [3]Oral and Maxillofacial Surgery, [4]Human Pathology, Graduate School, Tokyo Medical and Dental University, [5]Section of Molecular Genetics, Medical Research Institute, Tokyo Medical and Dental University, [6]Department of Genetic Diagnosis, Cancer Institute, Japanese Foundation for Cancer Research, [7]Section of Diagnostic Oral Pathology, Graduate School, Tokyo Medical and Dental University, and [8]Section of Molecular Pathophysiology, Graduate School of Allied Health Sciences, Tokyo Medical and Dental University, Tokyo, Japan

Date of submission 10 July 2009
Accepted for publication 26 April 2010

Sakamoto K, Aragaki T, Morita K-i, Kawachi H, Kayamori K, Nakanishi S, Omura K, Miki Y, Okada N, Katsube K-i, Takizawa T & Yamaguchi A

(2011) *Histopathology* **58**, 531–542

Down-regulation of keratin 4 and keratin 13 expression in oral squamous cell carcinoma and epithelial dysplasia: a clue for histopathogenesis

Aims: This study aimed to identify relevant keratin subtypes that may associate with the pathogenesis of oral epithelial neoplasms.

Methods and results: Expression of all the keratin subtypes was examined by cDNA microarray analysis of 43 oral squamous cell carcinoma (OSCC) cases. Immunohistochemical expression of the major keratins was examined in 100 OSCC and oral epithelial dysplasia (OED) cases. Many changes in keratin expression were observed and, significantly, consistent down-regulation of keratin 4 (K4) and K13 expression was observed. Aberrant expression of K4 and K13 was associated with morphological changes in the affected oral epithelium. Experiments with cell cultures transfected with various keratin subtypes suggested that alterations in keratin subtype expression can cause changes in cell shape and movement.

Conclusions: Aberrant expression of K4 and K13, which are the dominant pair of differentiation-related keratins in oral keratinocytes, indicates dysregulation of epithelial differentiation in OSCC and OED. These keratins, especially K4, may be useful for pathological diagnosis. We propose that the aberrant expression of K4 and K13 and concomitant up-regulation of the other keratins may be one of the causative factors for morphological alterations in the affected epithelium.

Keywords: cytokeratin, epithelial dysplasia, keratin, keratin 4, keratin 13, oral mucosa, squamous cell carcinoma

Abbreviations: EDTA, Tris/ethylenediamine tetraacetic acid; OED, oral epithelial dysplasia; OSCC, oral squamous cell carcinoma; SCC, squamous cell carcinoma

Introduction

Keratin is an intermediate filament cytoskeletal protein. The human genome contains 54 genes encoding functional keratins, of which 37 encode epithelial keratins and 17 encode hair keratins. Keratins can be divided into acidic and basic types; both types are coexpressed during the differentiation of epithelial tissues and arranged in heterotypic pairs to form chains of laterally aligned coiled-coil structure.[1] Because the composition

Address for correspondence: K Sakamoto, Section of Oral Pathology, Tokyo Medical and Dental University, Yushima 1-5-45, Bunkyo-ku, Tokyo 113-0034, Japan. e-mail: s-kei.mpa@tmd.ac.jp

of keratin pairs varies depending on cell type, differentiation status and environment, the assessment of the distribution of different keratin subtypes can facilitate cell typing and identification. Moreover, keratin subtyping is useful for cancer diagnosis, as cancer cells often exhibit abnormal keratin expression profiles.[1]

Several studies have indicated that some specific keratin subtypes are either down-regulated or up-regulated in oral squamous cell carcinoma (OSCC) and oral epithelial dysplasia (OED).[2–17] However, these studies have investigated limited numbers of selective keratin subtypes, and hence the results of different studies are often conflicting; this is probably because of the variations in the experimental procedures used, including the use of different antibodies. The correlation of each keratin subtype and its significance in pathogenesis has not been assessed fully.

In this study, we performed exhaustive keratin profiling to elucidate the comprehensive alterations in the expression of keratin subtypes in OSCC and OED.

Materials and methods

CLINICAL SPECIMENS

The surgical specimens from 43 patients with OSCC were collected for microarray analysis. The primary sites of cancer were tongue (18), gingiva (16), oral floor (five), buccal mucosa (three) and palate (one). Written informed consent was obtained from all the patients, and all the experimental procedures were approved by the Tokyo Medical and Dental University ethics committee. In addition, 100 specimens of OSCC and OED that were large enough to be sufficiently informative and contained normal epithelium were collected from the archives of the Dental Hospital at Tokyo Medical and Dental University. Grading of OED was performed according to the generally accepted criteria.[18]

CDNA MICROARRAY ANALYSIS

Cancer cells were isolated by laser capture microdissection. Squamous epithelial cells adjacent to OSCC were isolated from the specimens of nine patients as a normal control. Microarray analyses were performed as described previously.[19]

IMMUNOHISTOCHEMISTRY

Immunohistochemistry was performed according to the standard protocol. For antigen retrieval, the sections were placed in Tris/ethylenediamine tetraacetic acid (EDTA) buffer (10 mM Tris (pH = 9.0) and 1 mM EDTA) and autoclaved at 120°C for 20 min. The primary antibodies were anti-K1 (N-20; Santa Cruz, CA, USA), K2e (Ks2.342.7.1; Progen, Heidelberg, Germany), K4 (EP1599Y; Epitomics, Burlingame, CA, USA), K5 (XM26; Monosan, Uden, Netherlands), K6 (LHK6B; Neomarkers, Lab Vision, Fremont, CA, USA), K7 (RN7; Dako, Glostrup, Denmark), K8 (TS1; Novocastra, Leica Microsystems, Wetzlar, Germany), K9 (Ks9.70/Ks9.216; EuroDiagnostica, Malmö, Sweden), K10 (DE-K10; Neomarkers), K13 (KS-1A3; Novocastra), K14 (LL002; Abcam, Cambridge, MA, USA), K15 (EPR1614Y; Epitomics), K16 (LL025; Neomarkers), K17 (E3; Dako), K18 (DC10; Dako), K19 (EP1580Y; Epitomics), K20 (PW1; Dako) and hair keratins (AE13; Santa Cruz). Antimouse IgG-Alexafluor 594, anti-rabbit IgG-Alexafluor 488 (Invitrogen, Carlsbad, CA, USA), or Envision Dual link kit (Dako) was used as the secondary antibody. Evaluation of the expression was performed by comparing immunoreactivity in the lesion with that in the normal epithelium of the same specimen.

MOLECULAR CLONING OF KERATIN GENES

Human *K4* cDNA (IMAGE: 5453644) was purchased from Geneservice (Cambridge, UK). Human *K5*, *K13*, *K14* and *K17* cDNAs were synthesized by reverse transcriptase–polymerase chain reaction of RNA obtained from the gingiva of a male volunteer. *K4* and *K5* were cloned into pAcGFP1-C2 (Clontech, Mountain View, CA, USA) and *K13*, *K14* and *K17* were cloned into pDsRed-Monomer-N1 (Clontech). *Dominant negative K4* (*dnK4*), lacking the carboxyl terminal region (from S414 to R594), was the deletion construct of *K4*. Details of the cloning procedures will be provided upon request.

CELL CULTURE

HEK293T, Ca9-22 and U2OS cells were cultured in Dulbecco's modified Eagle's medium containing 10% fetal calf serum. Transfections were performed using FuGene6 (Roche Diagnostics, Basel, Switzerland BD Falcon, Franklin Lakes, NJ, USA). To assess the effect of different keratin expression on the cell motility, cells seeded in a Boyden chamber (pore size 8 μm; BD Falcon) were transfected with mock, K13 or K17 plasmid, and cell movement assay was performed as described previously.[20]

Results

CDNA MICROARRAY ANALYSIS OF OSCC

Expression level of the genes encoding each keratin subtype was represented as the mean of the signal

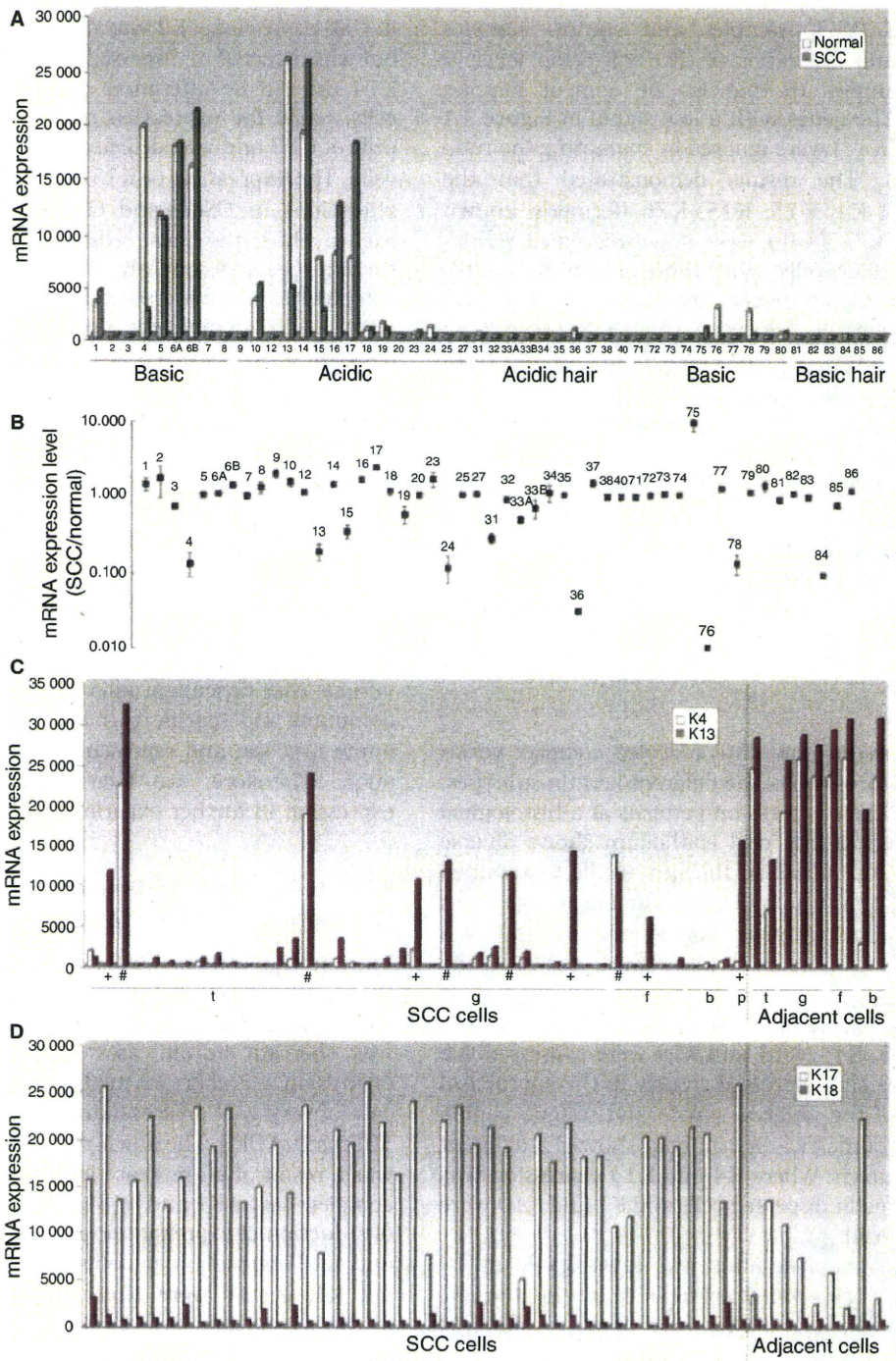

Figure 1. cDNA microarray analysis of oral squamous cell carcinoma (OSCC). **A.** The expressions of each keratin subtype in 43 OSCC samples and nine normal control samples are represented as the mean of the fluorescent signal intensity. Numerals in the horizontal axis denote the keratin subtypes. K1–K8 and K71–K80 are basic epithelial keratins. K9–K27 are acidic epithelial keratins. K31–K40 are acidic hair keratins and K81–K86 are basic hair keratins. Expressions of pseudogenes were omitted. **B.** The expression levels are represented as the ratios of the mean expression in OSCC to that in the normal samples. Error bars denote standard errors. Numerals denote the keratin subtypes. The vertical axis is logarithmic. **C.** The *K4* and *K13* signal intensities of each OSCC that arose in tongue (t), gingiva (g), oral floor (f), buccal mucosa (b) and palate (p). Nine samples to the right are the normal control samples. Crosses denote the cases with considerably retained expression of K13 but not K4. Sharps denote the cases with considerably retained expression of both K4 and K13. **D.** The K17 and K18 signal intensities of each case.

intensities of OSCC samples and control samples (Figure 1A) and the ratios of the expression level in the OSCC samples to that in the control samples (Figure 1B). The genes with a low signal in Figure 1A (for example, *K84*) were ignored in evaluating the ratio in Figure 1B. The results demonstrated that the expressions of K4, K13, K15, K76 (formerly known as K2b) and K78 (K5b) were down-regulated significantly in the OSCC cells, while those of K6b, K10, K14, K16, K17 and K75 (K6hf) were up-regulated. The down-regulation of K4 or K13 was observed in most cases (Figure 1C). Although many studies have reported up-regulation of K8 and K18 during oral carcinogenesis,[5,6,11,16,21,22] OSCC cases with elevated expression of K8, K18 were exceptional and their expression levels were low compared to those of the other keratins (data not shown and Figure 1D). In contrast, significant up-regulation of K17 was observed in most cases (Figure 1D).

IDENTIFICATION OF THE KERATINS WITH ALTERED EXPRESSION PATTERNS IN ORAL NEOPLASTIC LESIONS

Because the microarray data revealed complex variations in the expression of the different keratin subtypes, we examined their expression patterns at a histological level. Considering that oral epithelium shows diverse appearances depending on the site, we first examined the keratin expression profile in normal oral epithelium including tongue, gingiva, buccal mucosa and oral floor. Keratin expression profiles were basically the same throughout the oral cavity. K4 and K13 were expressed strongly in suprabasal cells, whereas in the basal cells, K5, K14, K15 and K19 were expressed. K6 and K16 were also expressed weakly in the suprabasal layer. Parts of the gingiva, palate and tongue papilla that are sites of masticatory mucosa showed a different expression pattern, where K4 and K13 expression was weakly detected in dispersed cells and K1 and K10 were expressed instead.

The expression of keratins was investigated in 10 cases of OSCC associated with OED in the tongue, gingiva, buccal mucosa and oral floor. A panel of keratin expression in a representative case is presented in the Supporting Information. K4 and K13 were significantly down-regulated or almost disappeared in OSCC and OED. K17, which was negative or faintly detected in normal mucosa, was up-regulated in the basal and suprabasal layer of most cases. K1 and K10 were also up-regulated considerably in the suprabasal layers of more than half of OSCC and OED cases. K6 and K16 were up-regulated diffusely in OSCC and also in OED of six cases. K2 was negative in normal mucosa but was detected in dispersed cells of two cases. K5 and K14 showed no alteration of expression in the basal cells, while the expression retained in the suprabasal cells of OED and was detected in virtually all the OSCC cells. The expression of K15 and K19 showed various alterations in OSCC and OED: both were expressed exclusively in the basal cells of normal epithelium but the expression frequently disappeared in OED, either completely or in dispersed cells. In OSCC, K15 and K19 were either completely negative or were detected diffusely or in dispersed cells. The immunohistochemical findings are summarised schematically in Figure 2A. Overall alteration of keratin expression revealed by microarray array analysis and immunohistochemistry is depicted schematically on a genome map (Figure 2B). These results confirmed the microarray data and highlighted relevant keratins to distinguish OED and OSCC from a normal epithelium. Among these, the down-regulation of K4 and K13 expression in lining mucosa was the most consistent. In contrast, expression of the other keratins showed various case-dependent alterations. K4 and K13 are a dominant and specific pair in suprabasal cells of oral lining mucosa, and represent their terminal differentiation. Therefore, we focused upon K4 and K13 expression in further experiments.

K4 AND K13 EXPRESSION ARE DOWN-REGULATED CONSISTENTLY IN OSCC AND OED

The immunohistochemical expression of K4 and K13 in OSCC and OED was investigated in an additional 90 cases (40 OSCCs and 50 OEDs) (Figure 3). K4 expression was aberrant in all cases of OSCC and OED. K13 expression was aberrant in all cases of OSCC, except one case of very well-differentiated SCC, and in 70% (35 of 50) cases of OED. The down-regulation of these proteins was a result of an increase in the number of cells with complete loss of K4 and K13 expression, and not a result of reduction of expression in individual cells. Loss of K4 and K13 expression usually occurred concomitantly, but K4(−) cells were often distributed more broadly in the lesions compared to K13(−) cells (Figure 3A,B). This suggests that the expression of K4 represents the terminal differentiation of oral keratinocytes more strictly than K13, and thus can be used as a more sensitive indicator for its dysregulation. In the OSCC lesions, most of the cancer cells were negative for both K4 and K13 expression (Figure 3A–C), although cancer nests with dispersed K4- and/or K13-positive cells were observed occasionally (Figure 3A). Using immunohistochemistry we investigated the cases in which a

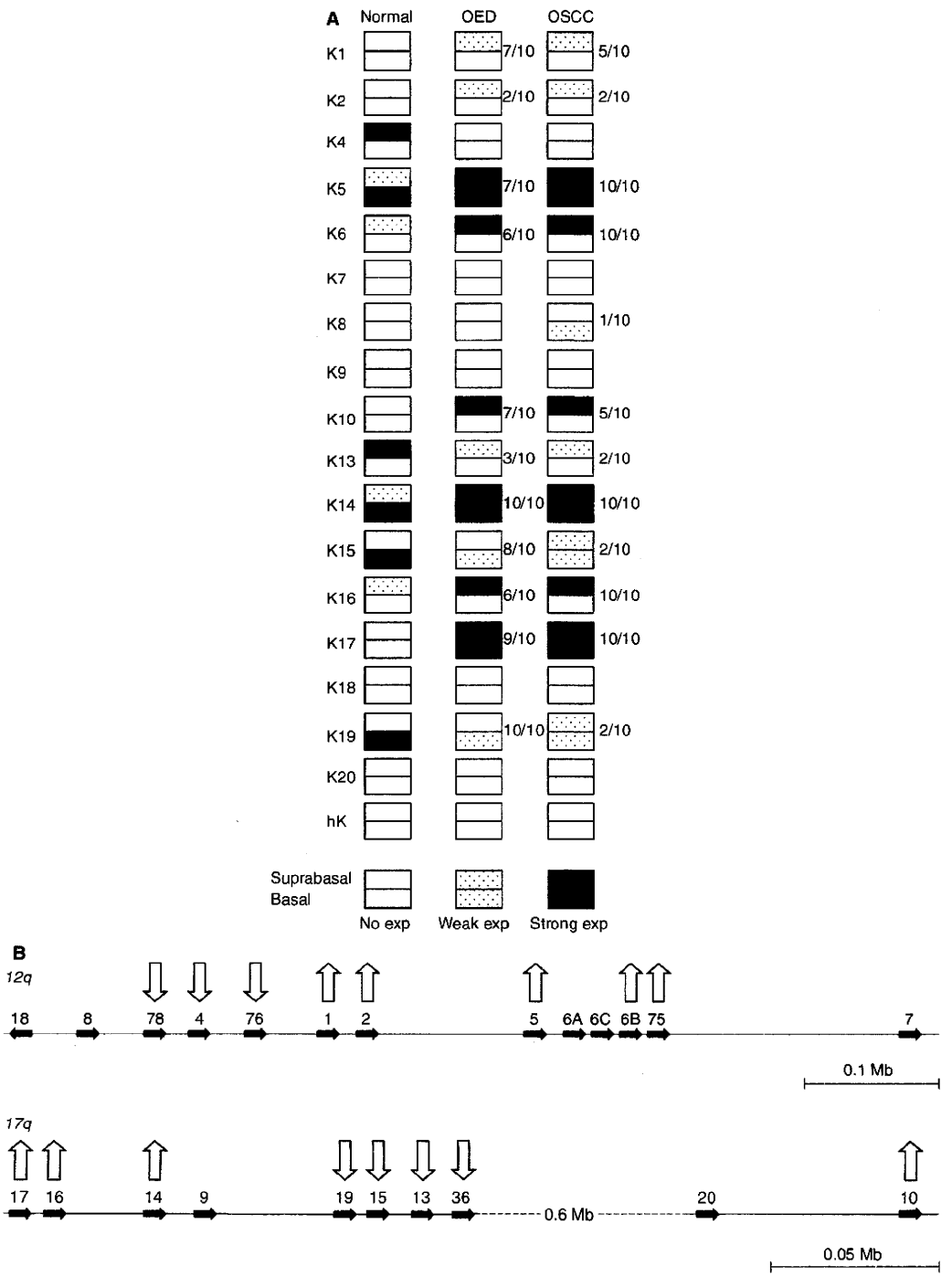

Figure 2. A. Schematic illustration of keratin expression profile in the normal oral mucosa, oral epithelial dysplasia (OED) and oral squamous cell carcinoma (OSCC). The epithelium is divided into basal and the suprabasal compartments and expression is represented by a three-grade evaluation. The black shading (strong expression) represents that the expression was observed strongly in virtually all cells in the positive case. The white shading (no expression) represents that the expression was almost completely negative in all the cases. The dotted shading (weak expression) represents that the expression was detected weakly or partially. The numbers of cases with an altered expression pattern is shown. B. Schematic illustration of the keratin loci, also showing keratins up-regulated (upward arrow) or down-regulated (downward arrow) in OSCC and OED. Only major epithelial keratins and keratins that exhibit significant changes of expression are depicted. The sizes of the genes are not shown.

considerably retained level of K4 or/and K13 expression was indicated by the microarray analysis (marked with '+' or '#', respectively, in Figure 1C), and confirmed that they also showed significant down-regulation of K4 and K13. This minor inconsistency between the microarray analysis and the immunohistochemical examination was due apparently to the sampling from the lesions in which K13-positive (and a few K4-positive) and K13-negative cancer nests coexisted.

In OED, K4 expression was absent or significantly down-regulated in all cases (Figure 3D). Both leucoplakic and erythroplakic lesions showed aberrant K4 expression, regardless of the grade of OED (Figure 3C,D). K13 was also down-regulated significantly in six of 16 cases of mild OED, 19 of 24 cases of moderate OED and all the cases of severe OED. A prominent feature in this observation was that aberrant K4 expression was always observed in a region that exhibited abnormal morphology (dysplasia) and was not observed in epithelium with normal appearance. As the adjacent epithelium usually showed normal K4 expression, the borders of K4 expression were clearly visible. At the periphery of the lesion, the distribution of K4(−) cells could be divided into two patterns:

Type 1
In a majority of cases (38 of 60), a definite border between the K4-positive and -negative regions was observed. The border of K13 expression matched that of K4 expression, although some K13(+) cells often remained in the K4(−) region. In this category, a clear histological demarcation between the normal epithelium and OED was visible, and the histological border coincided with the K4 expression border.

Type 2
In a minority of cases (22 of 60), there was a gradual increase in the number of K4(−) cells towards the centre of the lesion, forming a transition zone with a mixed population of K4-positive and K4-negative cells. In these cases, no distinct histological border was visible.

We examined the coexpression of K4 and K13 in individual cells by immunofluorescent double staining in 10 representative cases of OED. In the normal oral mucosa, suprabasal cells coexpressed both K4 and K13 (Figure 4A). In cases with Type 1 borders, K4(−)K13(−) cells were observed predominantly in the lesion with very few K4(−)K13(+) cells (Figure 4B). In the cases with Type 2 borders, the transition zones comprised mixed populations of K4(+)K13(+), K4(−)K13(−), and K4(−)K13(+) cells. In addition, a few cells with K4(+)K13(−) phenotype, which were never observed in the normal epithelia, were observed (Figure 4C).

PATHOPHYSIOLOGICAL ROLE OF ALTERED KERATIN EXPRESSION

Because the loss of K4 expression was correlated highly with the presence of OED, we hypothesized that aberrant expression of K4 and K13, with concomitant up-regulation of the other keratins, may be one cause of OED. To test this hypothesis, we transfected *K4*, *dnK4* and *K13* in Ca9-22 cells. The keratins were tagged with GFP (K4; green) or RFP (K13; red), allowing direct visualization of keratin filaments. DnK4 could form aggregates with a broad range of keratin subtypes, causing impaired keratin network formation (data not shown). Cotransfection of cognate keratin subtypes (i.e. *K4* and *K13*) resulted in a filamentous arrangement of each keratin subtype (Figure 5A). In contrast, cotransfection of *dnK4* with *K13* resulted in aggregation of both the keratin subtypes and the dnK4-expressing cells decreased in size, were round and showed poor adhesion to the surrounding cells (Figure 5A). These results implied that the impaired formation of a keratin network resulted in alteration in cell shape and attachment.

We next investigated whether K4 or K13 is functional in the absence of its cognate partner using the osteosarcoma cell line U2OS in which no keratins are expressed (data not shown). We transfected U2OS cells

Figure 3. K4 and K13 expression in oral squamous cell carcinoma (OSCC) and dysplasia (OED). A, Absence of K4 and K13 expression in well-differentiated squamous cell carcinoma (SCC) of tongue. Most of the cancer cells are negative for both K4 and K13. Some cancer nests contain K4(+) or K13(+) cells in a scattered fashion, where K13(+) cells are observed more than K4(+) cells. B, Absence of K4 and K13 expression in early SCC of tongue. The small dysplastic lesion between invasive cancer and normal epithelium shows absent K4 expression, and remaining but down-regulated expression of K13. C, A representative case of buccal SCC associated with epithelial dysplasia (OED) that was observed clinically as a mixture of erythroplakia and leucoplakia. High magnification views of selected areas are shown (a–f). The lesion exhibited various histological appearances. (a) Invasive squamous cell carcinoma. (b) Hyperparakeratosis and acanthosis with irregularly elongated rete ridges. (c) Weak keratinization and slightly bulbous rete ridges. (d) Orthokeratinization with minimal architectural and cellular atypia. (e) Weak keratinization with irregular shapes of rete ridges. (f) The periphery of the lesion, revealed by the expression of K4 and K13 as well as by histology. On the left, the affected epithelium is thin with little tendency to keratinization. K4 and K13 were down-regulated in all these lesions (a–f). D, Summary of the immunohistochemistry – a number of cases with distinct down-regulation of K4 or K13 are shown.

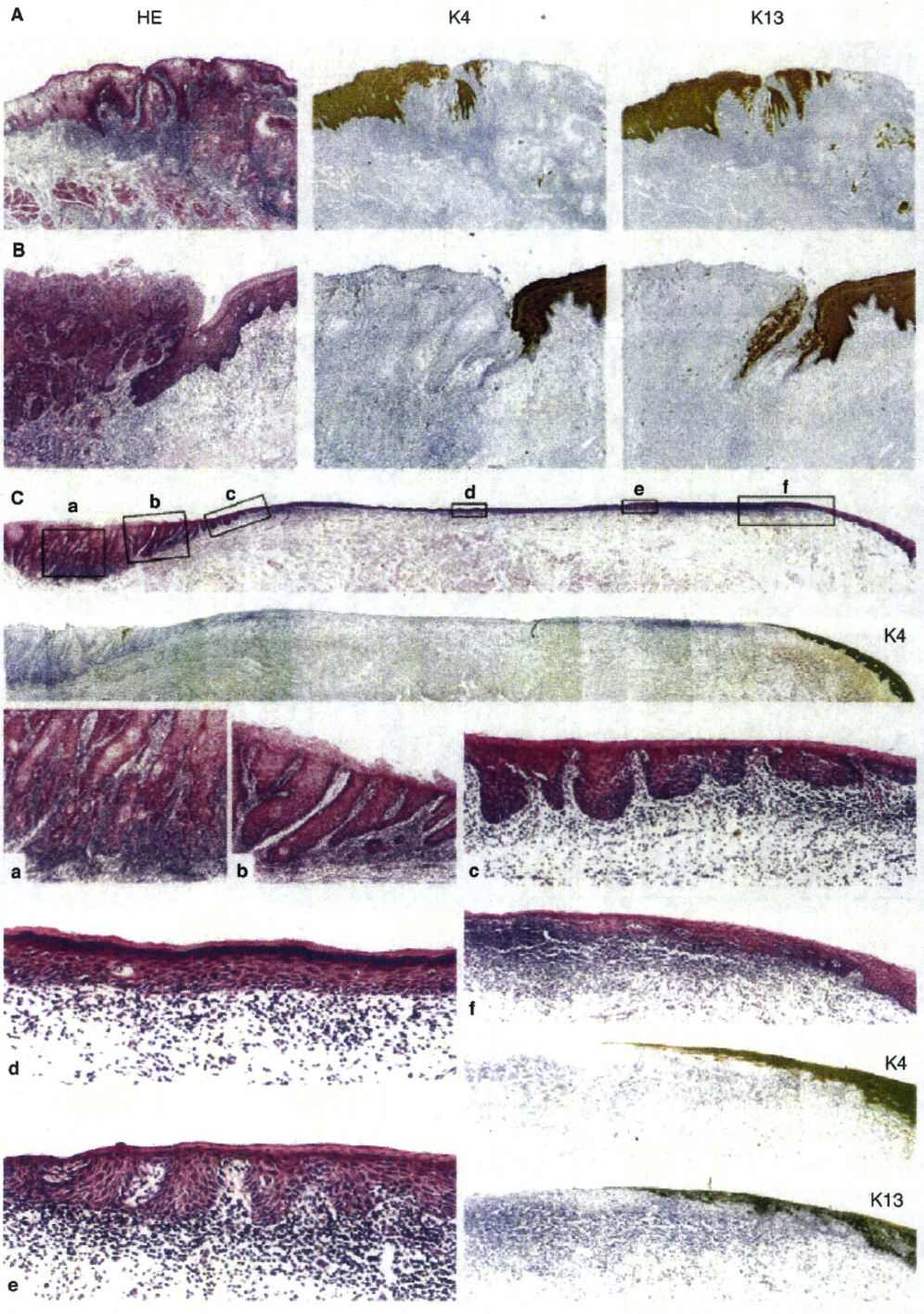

D

	OED			OSCC
	Mild	Moderate	Severe	
K4 ↓	16/16 (100%)	24/24 (100%)	10/10 (100%)	50/50 (100%)
K13 ↓	6/16 (38%)	19/24 (79%)	10/10 (100%)	49/50 (98%)

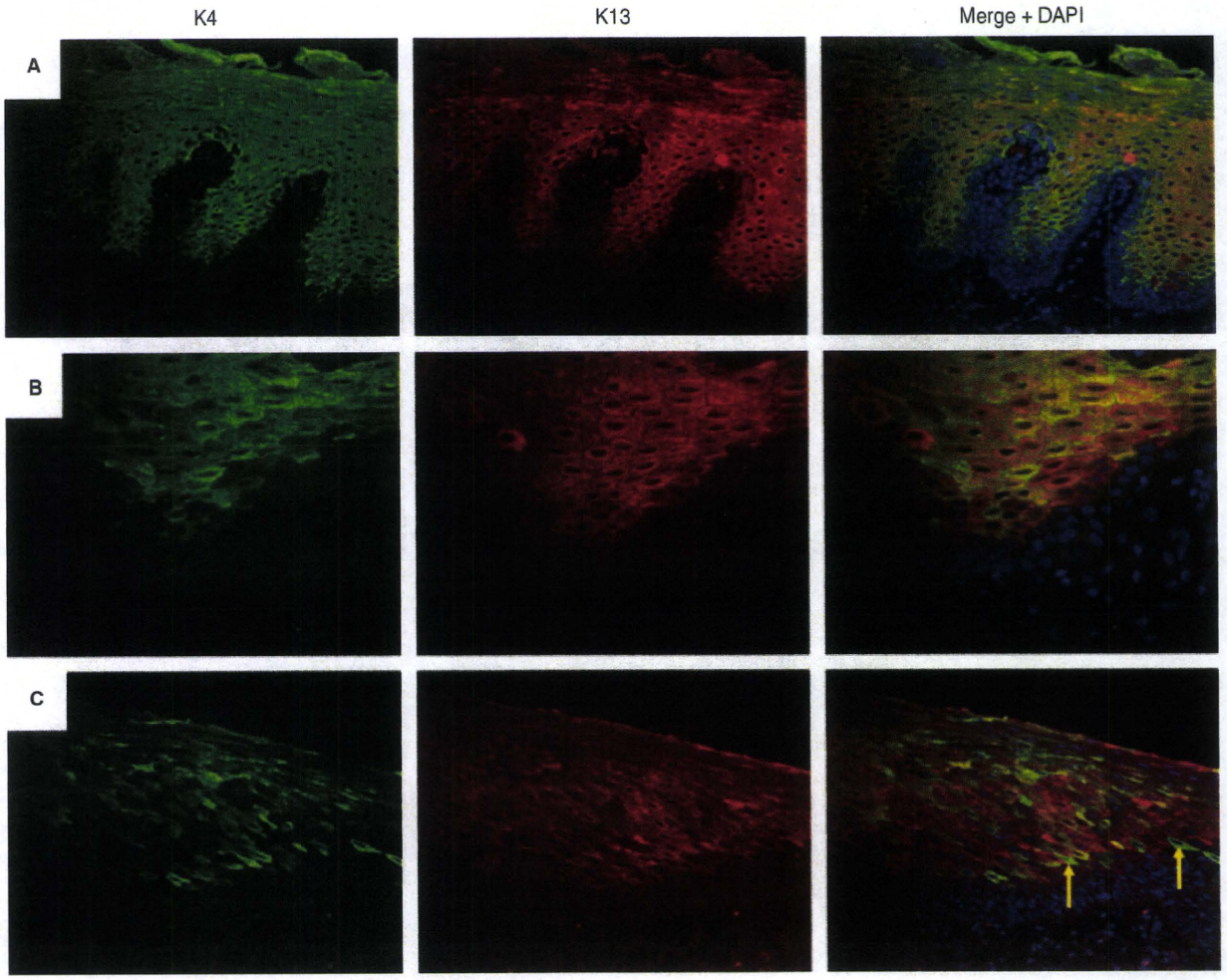

Figure 4. K4 and K13 expression in epithelial dysplasia (OED) revealed by immunofluorescent double staining. **A.** Normal epithelium with K4(+)K13(+) suprabasal cells. **B.** Mild OED with K4(−)K13(+) cells at the periphery of the lesion. **C.** Type 2 border of moderate OED showing a transition zone with a few K4(+)K13(−) cells (arrows).

with the genes of keratin subtypes: *K4*, *K5*, *K13* and *K14* and then examined the distribution of each keratin subtype. As shown in Figure 5B, basic keratins (K4 and K5) exhibited a filamentous network, whereas acidic keratins (K13 and K14) exhibited a diffuse distribution and lacked a filamentous network. This finding suggested that K13 and K14 were not functional in the absence of the basic keratins, although K4 and K5 were somehow integrated into the cytoskeletal network of the U2OS cells. These results suggested that aberrant expression of only one keratin subtype could cause an impaired cytoskeletal network. Nevertheless, a majority of the cells in OED retain relatively normal cytomorphology in the absence of K4 or K13 expression. We assumed that the other keratin subtypes that were induced ectopically could compensate for the loss of K4 or K13.

To test this hypothesis, we cotransfected the U2OS cells with different pairs of these keratins to investigate the mutual interaction of each keratin in the cytoskeletal network formation. Cotransfection with any of the combinations of keratin subtypes, i.e. K4/K13 (a cognate pair of differentiation-related keratins), K5/K14 (a cognate pair of basal cell keratins), K4/K14 and K5/K13, resulted in the formation of similar cytoskeletal network, as observed with the single-gene transfection of K4 or K5 (Figure 5B). This suggested that K5 and K14 could compensate for the function of K4 and K13, respectively, in the cytoskeletal network formation.

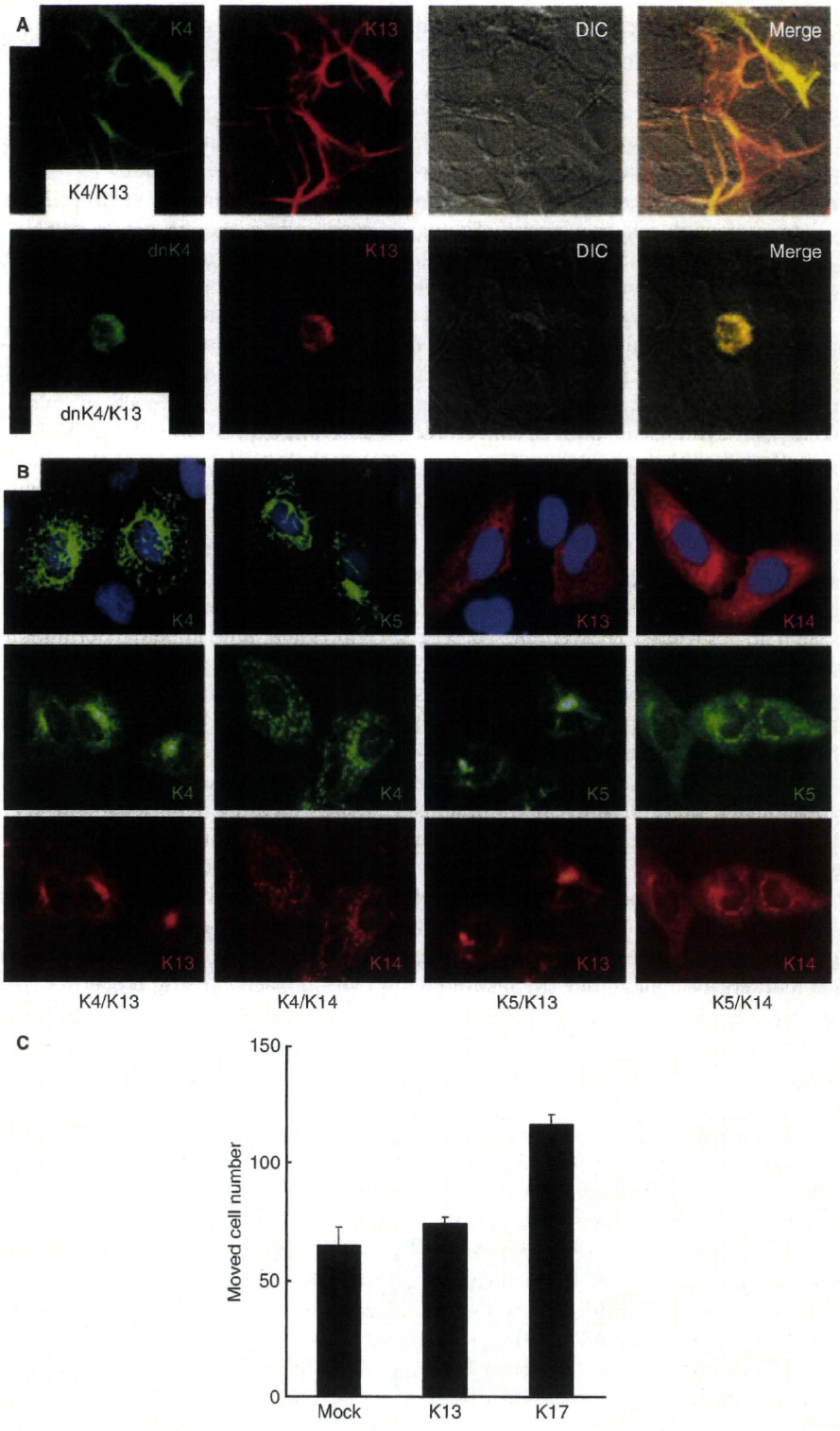

Figure 5. A. Ca9-22 cells cotransfected with *K4* or *dominant negative K4* (*dnK4*) and *K13*, tagged with GFP and RFP, respectively. B, K4/K14 or K5/K13 pairs are incorporated into the cytoskeletal networks similar to K4/K13 and K5/K14 pairs. U2OS cells were transfected with *GFP-K4*, *GFP-K5*, *K13-RFP* and *K14-RFP* at the indicated combination. C, Cell movement assay. HEK293T cells were transfected with a mock, K13 or K17 plasmid. After 24 h, the cells that moved to the external plate were counted. The results are the mean value of a triplicate experiment.

Finally, we examined the effect of keratin subtype expression on cell movement using a Boyden chamber assay. K17-transfected cells showed increased motility compared to mock- or K13-transfected cells (Figure 5C). This result implies that induction of K17 expression, which occurs in most cases of OSCC and OED, may lead to architectural alteration of the epithelium due to increased cell movement. Taking these results together with the *in situ* observations, demonstrating that the epithelia with aberrant K4 or/and K13 expression always exhibited morphological alterations, we assume that aberrant expression of these differentiation-related keratins and concomitant up-regulation of other keratins may be one of the causative factors for cytological and architectural alteration of the affected epithelium.

Discussion

We have demonstrated that features of K4 and K13 render them as relevant biomarkers for OED and OSCC. Distinct expression in individual cells enables precise and reliable evaluation; they are down-regulated consistently in OSCC and OED; and, because these keratins are major keratin pairs in the suprabasal cells of oral epithelium, their aberrant expression indicates abnormal terminal differentiation. As K4 was more sensitive and was down-regulated more broadly in the lesions than K13, we think that K4 is the first choice as a marker for dysregulation of oral epithelial differentiation. We compared the expression of K4 with that of Ki67 and TP53, and found that the usability of K4 was comparable to or even more sensitive than these commonly used markers for malignancy (K. Sakamoto, unpublished data). Combined usage of these markers for different cellular properties would facilitate more precise diagnosis.

OEDs are experienced commonly as a white patch (leukoplakia) or a red lesion (erythroplakia). Leukoplakia could be divided roughly into two groups on the basis of their keratin profiles. One was a K1(+)K10(+) lesion, in which the expressions of K4 and K13 were substituted for by their epidermal counterparts, K1 and K10, respectively, and the lesion exhibited an orthokeratotic appearance. The other was a K1(−)K10(−) lesion that typically showed hyperparakeratosis, although this keratosis was not achieved by original K4 and K13 pairs but by the other up-regulated keratins such as K5, K6, K14, K16, and especially K17. When little expression of the differentiation-related keratins was induced, the lesion led to poor development of the prickled cell layer, exhibiting an erythroplakic appearance (unpublished data). These are examples of the direct correlation between alteration of keratin expression and changes in the epithelial morphology. In any case, down-regulation of K4 and K13 seemed essential as we never observed the other keratins up-regulation in the presence of normal expression of K4 and K13.

Missense mutations in either *K4* and *K13* genes can cause white sponge nevus (WSN).[23,24] Furthermore, *K4* knockout mice show a cellular phenotype that resembles epithelial dysplasia in humans, including hyperkeratosis, atypical nuclei and cell degeneration.[25] Although commonly experienced OED usually show somewhat different histological features from that of WSN and the K4-knockout mice, these imply that aberrant expression of K4 or K13 may lead possibly to morphological change of the affected epithelium. We have demonstrated that regions with aberrant K4 and K13 expression coincide with altered epithelial morphology, including the concurrent formation of a histological border with a K4-expression border. Cell culture experiments suggest that aberrant keratin expression and impaired formation of a cytoskeletal network could cause changes in cell shape. This may not be a dominant factor for alteration of the whole epithelial morphology, because other keratins are usually induced in order to compensate for the absence of the original keratins. Rather, increased cell motility represented by K6, K16 and K17 expression may associate with architectural alterations. These keratins are induced robustly in a hyperproliferative epithelium after injury, and their presence correlates with changes in the morphology of epithelial cells at a wound edge.[26] Forced expression of K16 in progenitor skin keratinocytes impacts directly properties such as adhesion and migration.[27] Our results demonstrate that forced expression of K17 leads to increased cell migration. Altogether, we assume that alteration of keratin subtype expression is one of the factors that underlie cytological and architectural alterations observed in OED and OSCC. If so, keratin profiling is not only a practical but also a rational aid for pathological diagnosis.

The upstream factors that initiate changes in keratin subtype expression in the oral mucosa are currently unknown. We examined immunohistochemically several factors that reportedly regulate keratinocyte differentiation, such as p63, FoxN1, AKT, ERK, FAK and integrins, but none showed a correlation with K4 and K13 expression (data not shown). A high correlation between K4 and K13 expression patterns suggests the presence of a common mechanism to regulate their transcription, but little sequence homology was found in their promoter regions (data not

shown). The well-coordinated regulation of multiple keratin expression may be associated with the unique genome organization of keratin genes. Basic and acidic keratin genes, except *K18* (which locates on *12q* back to back with K8), are aligned tandemly on *12q* and *17q*, respectively, and this genomic organization is evolutionarily well conserved. Our comprehensive keratin profiling reveals that each of the up-regulated and down-regulated keratins in OSCC and OED is clustered on the genome (Figure 2B). This implies that the epigenetic status of keratin loci may be important for the selective expression of specific repertoires of keratins. In this sense, analysis of methylation states in the keratin loci would be an interesting future project for understanding the coordinated expression of different keratin subtypes.

In conclusion, our study demonstrated that aberrant expression of K4 and K13, which are differentiation-related keratins in oral keratinocytes, is the most essential feature observed in OSCC and OED.

Acknowledgements

This work was supported by a grant-in-aid from the Japanese Ministry of Education, Culture, Sports, Science and Technology (KAKENHI 21592320). The authors thank Miwako Hamagaki and Kiyoko Nagumo for technical assistance and undergraduate students Yuhei Ikeda and Ryushiro Sugita for their contributions to this study.

References

1. Moll R, Divo M, Langbein L. The human keratins: biology and pathology. *Histochem. Cell Biol.* 2008; **129**: 705–733.
2. Crowe DL, Milo GE, Shuler CF. Keratin 19 downregulation by oral squamous cell carcinoma lines increases invasive potential. *J. Dent. Res.* 1999; **78**: 1256–1263.
3. Farrar M, Sandison A, Peston D, Gallani M. Immunocytochemical analysis of AE1/AE3, CK 14, Ki-67 and p53 expression in benign, premalignant and malignant oral tissue to establish putative markers for progression of oral carcinoma. *Br. J. Biomed. Sci.* 2004; **61**: 117–124.
4. Fillies T, Werkmeister R, Packeisen J *et al.* Cytokeratin 8/18 expression indicates a poor prognosis in squamous cell carcinomas of the oral cavity. *BMC Cancer* 2006; **6**: 10.
5. Gires O, Mack B, Rauch J, Matthias C. CK8 correlates with malignancy in leukoplakia and carcinomas of the head and neck. *Biochem. Biophys. Res. Commun.* 2006; **343**: 252–259.
6. Matthias C, Mack B, Berghaus A, Gires O. Keratin 8 expression in head and neck epithelia. *BMC Cancer* 2008; **8**: 267.
7. Ogden GR, Lane EB, Hopwood DV, Chisholm DM. Evidence for field change in oral cancer based on cytokeratin expression. *Br. J. Cancer* 1993; **67**: 1324–1330.
8. Ohkura S, Kondoh N, Hada A *et al.* Differential expression of the keratin-4, -13, -14, -17 and transglutaminase 3 genes during the development of oral squamous cell carcinoma from leukoplakia. *Oral Oncol.* 2005; **41**: 607–613.
9. Su L, Morgan PR, Lane EB. Keratin 14 and 19 expression in normal, dysplastic and malignant oral epithelia. A study using *in situ* hybridization and immunohistochemistry. *J. Oral Pathol. Med.* 1996; **25**: 293–301.
10. Toyoshima T, Vairaktaris E, Nkenke E, Schlegel KA, Neukam FW, Ries J. Cytokeratin 17 mRNA expression has potential for diagnostic marker of oral squamous cell carcinoma. *J. Cancer Res. Clin. Oncol.* 2008; **134**: 515–521.
11. Xu XC, Lee JS, Lippman SM, Ro JY, Hong WK, Lotan R. Increased expression of cytokeratins CK8 and CK19 is associated with head and neck carcinogenesis. *Cancer Epidemiol. Biomarkers Prev.* 1995; **4**: 871–876.
12. Yanagawa T, Yoshida H, Yamagata K *et al.* Loss of cytokeratin 13 expression in squamous cell carcinoma of the tongue is a possible sign for local recurrence. *J. Exp. Clin. Cancer Res.* 2007; **26**: 215–220.
13. Zhong LP, Chen WT, Zhang CP, Zhang ZY. Increased CK19 expression correlated with pathologic differentiation grade and prognosis in oral squamous cell carcinoma patients. *Oral Surg. Oral Med. Oral Pathol. Oral Radiol. Endod.* 2007; **104**: 377–384.
14. Depondt J, Shabana AH, Sawaf H, Gehanno P, Forest N. Cytokeratin alterations as diagnostic and prognostic markers of oral and pharyngeal carcinomas. A prospective study. *Eur. J. Oral Sci.* 1999; **107**: 442–454.
15. Fillies T, Jogschies M, Kleinheinz J, Brandt B, Joos U, Buerger H. Cytokeratin alteration in oral leukoplakia and oral squamous cell carcinoma. *Oncol. Rep.* 2007; **18**: 639–643.
16. Ogden GR, Chisholm DM, Adi M, Lane EB. Cytokeratin expression in oral cancer and its relationship to tumor differentiation. *J. Oral Pathol. Med.* 1993; **22**: 82–86.
17. Vaidya MM, Borges AM, Pradhan SA, Bhisey AN. Cytokeratin expression in squamous cell carcinomas of the tongue and alveolar mucosa. *Eur. J. Cancer B Oral Oncol.* 1996; **32B**: 333–336.
18. Barnes L, Eveson J, Reichart P, Sidransky D. Epithelial precursor lesions. *World Health Organization classification of tumours. Pathology and genetics. Head and neck tumours.* Geneva, Switzerland: WHO Press, 2005; 177–180.
19. Tomioka H, Morita K, Hasegawa S, Omura K. Gene expression analysis by cDNA microarray in oral squamous cell carcinoma. *J. Oral Pathol. Med.* 2006; **35**: 206–211.
20. Bonifacino JS, Dasso M, Harford JB, Lippincott-Schwartz J, Yamada KM. *Current protocols in cell biology.* Hoboken, NJ, USA: John Wiley and Sons, Inc., 2007.
21. Su L, Morgan PR, Lane EB. Protein and mRNA expression of simple epithelial keratins in normal, dysplastic, and malignant oral epithelia. *Am. J. Pathol.* 1994; **145**: 1349–1357.
22. Zhong LP, Zhao SF, Chen GF, Ping FY, Xu ZF, Hu JA. Increased levels of CK19 mRNA in oral squamous cell carcinoma tissue detected by relative quantification with real-time polymerase chain reaction. *Arch. Oral Biol.* 2006; **51**: 1112–1119.
23. Richard G, De Laurenzi V, Didona B, Bale SJ, Compton JG. Keratin 13 point mutation underlies the hereditary mucosal epithelial disorder white sponge nevus. *Nat. Genet.* 1995; **11**: 453–455.
24. Rugg EL, McLean WH, Allison WE *et al.* A mutation in the mucosal keratin K4 is associated with oral white sponge nevus. *Nat. Genet.* 1995; **11**: 450–452.
25. Ness SL, Edelmann W, Jenkins TD, Liedtke W, Rustgi AK, Kucherlapati R. Mouse keratin 4 is necessary for internal epithelial integrity. *J. Biol. Chem.* 1998; **273**: 23904–23911.

26. Mazzalupo S. Wong P. Martin P. Coulombe PA. Role for keratins 6 and 17 during wound closure in embryonic mouse skin. *Dev. Dyn.* 2003; **226**; 356–365.
27. Wawersik M. Coulombe PA. Forced expression of keratin 16 alters the adhesion. differentiation. and migration of mouse skin keratinocytes. *Mol. Biol. Cell* 2000; **11**; 3315–3327.

Supporting Information

Additional Supporting Information may be found in the online version of this article:

Figure S1. A panel indicating the major keratin expression pattern in a case of oral squamous cell carcinoma of tongue.

Please note: Wiley-Blackwell are not responsible for the content or functionality of any supporting materials supplied by the authors. Any queries (other than missing material) should be directed to the corresponding author for the article.

Maf promotes osteoblast differentiation in mice by mediating the age-related switch in mesenchymal cell differentiation

Keizo Nishikawa,[1,2] Tomoki Nakashima,[1,2,3] Shu Takeda,[4] Masashi Isogai,[5] Michito Hamada,[5] Ayako Kimura,[4] Tatsuhiko Kodama,[6] Akira Yamaguchi,[7] Michael J. Owen,[8] Satoru Takahashi,[5] and Hiroshi Takayanagi[1,2,3]

[1]Department of Cell Signaling, Graduate School of Medical and Dental Sciences, Tokyo Medical and Dental University, Tokyo, Japan. [2]Global Center of Excellence Program, International Research Center for Molecular Science in Tooth and Bone Diseases, and [3]Japan Science and Technology Agency, ERATO, Takayanagi Osteonetwork Project, Tokyo, Japan. [4]Department of Orthopaedic Surgery, Graduate School of Medical and Dental Sciences, Tokyo Medical and Dental University, Tokyo, Japan. [5]Institute of Basic Medical Sciences and Laboratory Animal Resource Center, University of Tsukuba, Tsukuba, Japan. [6]Department of Molecular Biology and Medicine, Research Center for Advanced Science and Technology, University of Tokyo, Tokyo, Japan. [7]Department of Oral Pathology, Graduate School of Medical and Dental Sciences, Tokyo Medical and Dental University, Tokyo, Japan. [8]GlaxoSmithKline, Stevenage, United Kingdom.

Aging leads to the disruption of the homeostatic balance of multiple biological systems. In bone marrow multipotent mesenchymal cells undergo differentiation into various anchorage-dependent cell types, including osteoblasts and adipocytes. With age as well as with treatment of antidiabetic drugs such as thiazolidinediones, mesenchymal cells favor differentiation into adipocytes, resulting in an increased number of adipocytes and a decreased number of osteoblasts, causing osteoporosis. The mechanism behind this differentiation switch is unknown. Here we show an age-related decrease in the expression of *Maf* in mouse mesenchymal cells, which regulated mesenchymal cell bifurcation into osteoblasts and adipocytes by cooperating with the osteogenic transcription factor Runx2 and inhibiting the expression of the adipogenic transcription factor *Pparg*. The crucial role of Maf in both osteogenesis and adipogenesis was underscored by in vivo observations of delayed bone formation in perinatal *Maf*$^{-/-}$ mice and an accelerated formation of fatty marrow associated with bone loss in aged *Maf*$^{+/-}$ mice. This study identifies a transcriptional mechanism for an age-related switch in cell fate determination and may provide a molecular basis for novel therapeutic strategies against age-related bone diseases.

Introduction

A progressive and irreversible accumulation of DNA damage, which is triggered by telomere shortening and various stressors such as oxidative stress, contributes to cellular senescence and organismal aging (1, 2), but how aging is related to the disruption of the homeostatic balance of cell differentiation from a common progenitor is not well understood. Bone marrow contains multipotent mesenchymal progenitor cells, which differentiate into various anchorage-dependent cell types, including adipocytes and osteoblasts (3, 4). With age, mesenchymal cells in the bone marrow become inclined to undergo differentiation into adipocytes rather than osteoblasts (5–7), resulting in an increased number of adipocytes and a decreased number of osteoblasts, causing osteoporosis. Adipocytes are also known to directly inhibit functions of other cells in the bone marrow, including hematopoietic stem cells and osteoblasts (8–11). Since an increase in marrow fat along with bone loss is observed in diabetic patients treated with thiazolidinediones (TZDs) (12), understanding the mechanism of this differentiation switch has substantial relevance to both the management of age-related osteoporosis and secondary osteoporosis after such drug treatment. However, the change in mesenchymal cell differentiation cannot be adequately explained by cellular senescence or the cell cycle arrest caused by DNA damage. While estrogen deficiency causes postmenopausal osteoporosis (6, 13), it has been suggested that the downregulation of cytokines and hormones, such as IGF1, TGFB1, IL-11, and growth hormone, is correlated with age-related bone loss (6, 14, 15). However, a cell-intrinsic mechanism that regulates the age-related switch in mesenchymal cell differentiation remains to be elucidated. Here we report an age-related decrease in the expression of *Maf* in mesenchymal cells and present evidence that Maf regulates mesenchymal cell bifurcation into osteoblasts and adipocytes. This study establishes the crucial role of the Maf-mediated transcriptional program in the physiological and age-related regulation of mesenchymal cell lineage, which may facilitate the development of new therapeutic strategies against bone and metabolic diseases.

Results

A genome-wide screening of transcription factors involved in the age-related decrease in bone formation. To identify the transcription factors involved in age-related bone loss, we performed a genome-wide screening of mRNAs expressed in cells derived from mouse calvaria during osteoblastogenesis. Among 1,470 transcription factors, we identified 163 genes related to osteogenic function; the identifying characteristic of these factors was that their expression was increased by more than 4-fold during osteoblastogenesis (Figure 1A and Supplemental Table 1, A and B; supplemental material

Conflict of interest: The authors have declared that no conflict of interest exists.
Citation for this article: *J Clin Invest.* 2010;120(10):3455–3465. doi:10.1172/JCI42528.

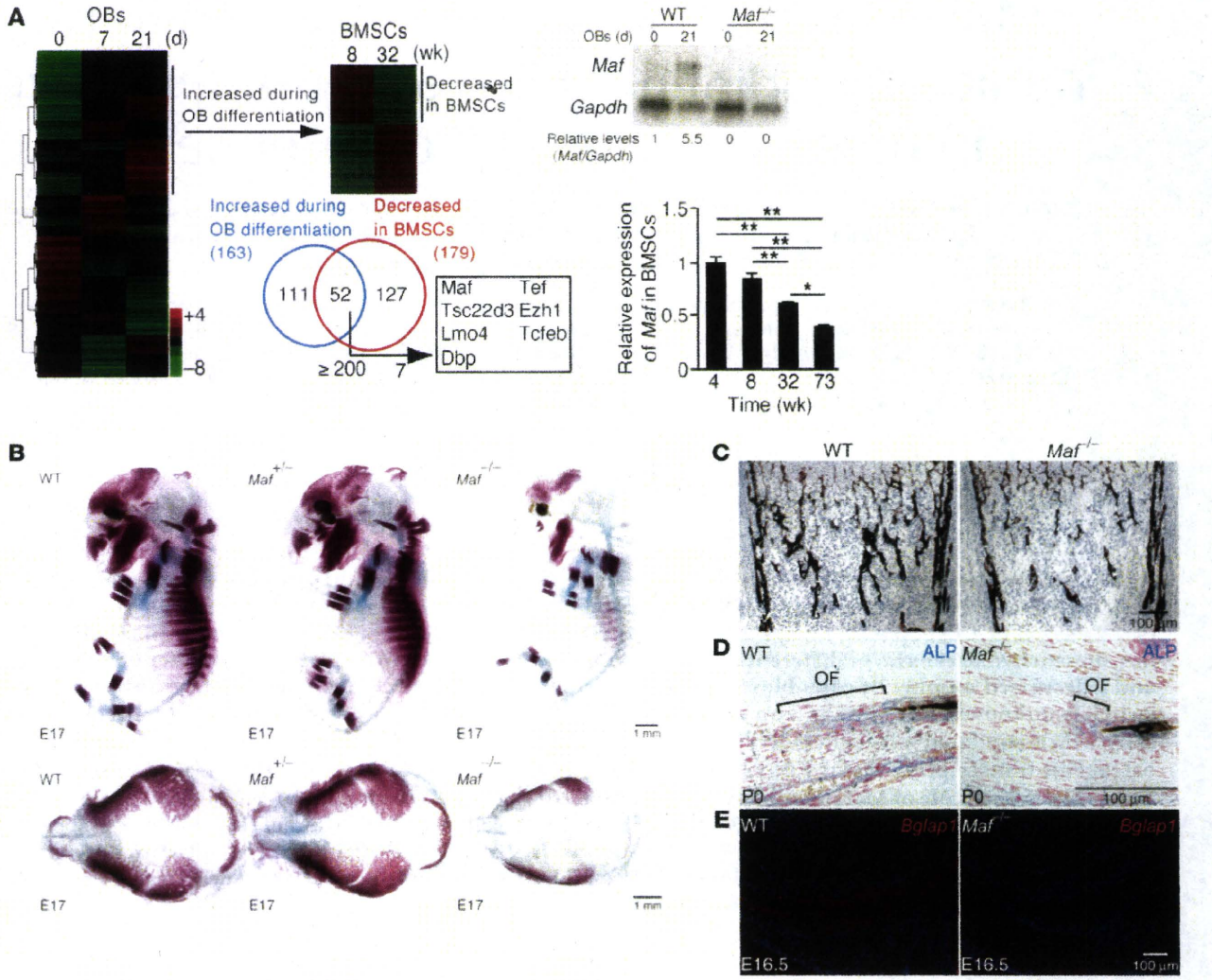

Figure 1

Impaired bone formation in *Maf*$^{-/-}$ mice. (**A**) A genome-wide screening of transcription factor mRNAs during in vitro differentiation of osteoblasts (OBs) and a comparison of their expression between 8- and 32-week-old BMSCs. The increase in *Maf* expression during osteoblastogenesis was confirmed in calvarial osteoblasts (RNA blot analysis, right top). *Maf* expression was markedly lower in BMSCs derived from the aged mice (real-time RT-PCR analysis, right bottom). Screening results are summarized in the Venn diagram. $^{*}P < 0.05$; $^{**}P < 0.01$. (**B**) Alizarin red/alcian blue staining of E17 embryos (top). Top view of calvaria (bottom). Images in **B** are composites. (**C**) Histology (von Kossa staining) and micro-computed tomography analysis of WT and *Maf*$^{-/-}$ littermates at P0 ($n = 3$). Scale bar: 100 μm. (**D**) ALP and von Kossa staining of osteogenic fronts (OFs) in the calvaria of WT and *Maf*$^{-/-}$ littermates. Scale bar: 100 μm. (**E**) Expression of *Bglap1* in the calvaria of WT and *Maf*$^{-/-}$ mice (in situ hybridization). Scale bar: 100 μm.

available online with this article; doi:10.1172/JCI42528DS1). To identify age-related genes, we also comprehensively analyzed the mRNAs expressed by bone marrow stromal cells (BMSCs) derived from 8- and 32-week-old mice, which resulted in identifications of 179 genes, the expression of which was decreased in the aged mice by more than 2 fold (Supplemental Table 1C). Fifty-two genes met both criteria (Supplemental Table 1D), from which we selected 7 genes preferentially expressed in BMSCs (with an average difference greater than 200). Among these 7 genes, we identified *Maf* (also known as c-Maf) to be the most highly expressed in the BMSCs. We confirmed that the expression of *Maf* increased during osteoblastogenesis, using calvarial and BMSCs (Figure 1A, right top, and Supplemental Figure 1A), and decreased with age (Figure 1A, right bottom, and Supplemental Figure 1B). Maf, a basic leucine zipper transcription factor, is known to be involved in the regulation of diverse developmental processes such as lens fiber elongation (16) and Th2 cell differentiation (17, 18). Although it has been documented that transcription factors such as ΔFosb, Taz, Esr1, Msx2, and Cebpβ regulate the bifurcation of osteoblast/adipocyte differentiation (7, 19, 20), the expression of ΔFosb was increased in aged BMSCs (Supplemental Figure 2) and the other 4 factors were not included in the 179 age-related genes (Supplemental Table 1C). These results suggest that Maf is one of the potential candidate genes underlying an age-related decrease in osteoblastogenesis.

The indispensable role of Maf in osteogenesis. Since *Maf*$^{-/-}$ mice usually die immediately after birth (16), we investigated the role of Maf in osteogenesis by analyzing the skeletal development of perinatal

Table 1
Skeletal development of perinatal *Maf*$^{-/-}$ mice

	WT	*Maf*$^{-/-}$
BV/TV (%)	29.51 ± 0.15	23.56 ± 0.32[A]
Tb.N (mm^{-1})	13.43 ± 0.26	11.81 ± 0.33[B]
Tb.Sp (μm)	51.86 ± 1.59	64.98 ± 1.46[A]
Tb.Th (μm)	22.47 ± 0.03	20.36 ± 0.63[B]

Microcomputed tomography analysis of WT and *Maf*$^{-/-}$ littermates at P0. BV/TV, bone volume/tissue volume, Tb.N, trabecular number, Tb.Sp, trabecular separation, and Tb.Th, trabecular thickness. [A]$P < 0.01$. [B]$P < 0.05$.

Maf$^{-/-}$ mice. Bone formation was severely impaired in both the long and calvarial bones in the embryos of *Maf*$^{-/-}$ mice (Figure 1B), and bone volume was decreased in newborn *Maf*$^{-/-}$ mice (Figure 1C, Table 1, and Supplemental Figure 3). The formation of alkaline phosphatase–positive (ALP-positive) cells on an osteogenic front was markedly impaired in the calvaria of newborn *Maf*$^{-/-}$ mice (Figure 1D). In situ hybridization analysis revealed the expression of osteoblast genes, such as *Bglap1* (encoding osteocalcin), but not of *Runx2* was much lower in the embryos of *Maf*$^{-/-}$ mice than WT mice (Figure 1E and Supplemental Figure 4, A and B), although the proliferating or apoptotic osteoblast numbers were not different (Supplemental Figure 4C). Since the osteoclast number was decreased in *Maf*$^{-/-}$ mice, possibly in a cell-autonomous manner (Supplemental Figure 5), it is unlikely that abnormal osteoclastic bone resorption contributes to the low bone mass phenotype in *Maf*$^{-/-}$ mice. When a neomycin-resistance gene cassette was inserted into the *Maf* locus, chondrocyte development was reported to be affected in the mutant mice, but the mice were not perinatally lethal (18). In the current study, in which the coding sequence of Maf was entirely replaced by the *LacZ* cassette, the mice were perinatally lethal and exhibited more severe chondrocyte abnormalities (Supplemental Figure 6). It is difficult to rule out the possibility that a defect in chondrocytes contributes to a skeletal phenotype in long bone, but *Maf*$^{-/-}$ mice exhibited a defective bone formation in flat bones, like the calvaria (Figure 1B), which are not formed by endochondral bone formation, suggesting a role of Maf in osteoblasts. To analyze a cell-autonomous defect in osteoblasts further, osteoblast differentiation was evaluated in an in vitro culture system of osteoblast precursor cells derived from the calvaria of newborn *Maf*$^{-/-}$ mice. ALP activity and bone nodule formation were markedly suppressed in *Maf*$^{-/-}$ cells (Figure 2A), but neither the proliferation nor apoptosis was affected (Figure 2B). These results collectively indicate that a complete lack of *Maf* led to an osteopenic phenotype, due to impaired osteoblast differentiation and bone formation.

Maf regulates osteoblast differentiation in cooperation with Runx2. The expression of various osteoblast-specific genes, including *Bglap1*, was severely suppressed in *Maf*$^{-/-}$ cells (Figure 2, C and D), but *Runx2*, a well-known transcriptional regulator of *Bglap1* (21, 22), was normally expressed in *Maf*$^{-/-}$ mice (Supplemental Figure 4B). It is notable that *Maf* expression was not decreased in *Runx2*$^{-/-}$ calvarial osteoblasts (Supplemental Figure 7). These results prompted us to investigate whether Maf directly regulates the *Bglap1* promoter. As expected, 5 Maf recognition element–like (MARE-like) sequences were contained in the 1,050-base *Bglap1* promoter region (Figure 2E). A reporter gene assay indicated that Maf activates the *Bglap1* promoter mainly through a region containing 3 proximal MARE-like sequences (MARE1–MARE3), which was included in the proximal DNase hypersensitive site (23) and partially overlapped with osteoblast-specific element 1 (OSE1) (22) (Figure 2F). ChIP experiments showed that Maf is recruited to the region containing MARE1–MARE3 in primary osteoblasts (Figure 2G), suggesting that Maf directly regulates the *Bglap1* promoter.

To gain insight into the transcriptional partners of Maf, we analyzed the Maf transcriptional network using a systems biology approach, based on protein-protein interaction databases and our own GeneChip analysis. Fos, Jun, Atf4, Nfat, and Runx2 were included among the transcription factors predicted to interact with Maf (Supplemental Figure 8). The function of these candidate partners was examined in the Maf-mediated activation of the *Bglap1* promoter, which was found to be exclusively enhanced by the addition of Runx2 (Figure 2H and data not shown). Consistent with this, the transcriptional activity of Maf on the *Bglap1* promoter was markedly decreased in *Runx2*$^{-/-}$ cells (Supplemental Figure 9). Maf bound to Runx2 in an immunoprecipitation assay (Figure 3 and Supplemental Figure 10), and immunohistochemical analysis showed that Maf was colocalized with Runx2 in calvarial osteoblasts (Supplemental Figure 11). Thus, these results suggest that Maf controls osteoblast differentiation by regulating osteoblastic gene expression mainly in cooperation with Runx2.

Maf suppresses adipogenesis by the downregulation of Pparg. We further characterized the *Maf*$^{-/-}$ calvarial cells using gene set enrichment analysis (GSEA), which revealed adipocyte-related genes to be highly enriched in *Maf*$^{-/-}$ cells (Supplemental Figure 12). Indeed, GeneChip data showed that the expression of adipocyte genes was upregulated in *Maf*$^{-/-}$ calvarial cells, even under the conditions optimized for osteoblast differentiation (Figure 4A). *Maf*$^{-/-}$ cells differentiated into oil red O–positive adipocytes more efficiently than WT cells (Figure 4B). Real-time RT-PCR analysis confirmed the expression of *Pparg*, the key transcription factor for adipogenesis, as well as that of *Fabp4*, *Slc2a4*, *Lpl*, *Acc1*, and *Cd36*, downstream effectors of Pparγ (24–26), to be markedly elevated in *Maf*$^{-/-}$ cells (Figure 4C and Supplemental Figure 13). To further investigate the role of Maf in osteoblast and adipocyte differentiation, we ectopically expressed Maf in C3H10T1/2 cells, a stromal cell line with a capacity to differentiate into both osteoblasts and adipocytes, and found that the introduction of Maf resulted in a severe blockade of adipocyte differentiation and an enhancement of osteoblast differentiation (Figure 4D and Supplemental Figure 14). Similar results were obtained using another stromal cell line, ST2, and BMSCs (Supplemental Figure 15, A–C). In addition, short hairpin RNA-mediated knockdown of Maf in ST2 cells resulted in a blockade of osteoblast differentiation and an acceleration of adipocyte differentiation (Supplemental Figure 15, D and E). Similar results were obtained using BMSCs (Supplemental Figure 15F). These results suggest that Maf promotes osteoblast differentiation and inhibits adipocyte differentiation in a cell-autonomous manner.

To understand the mechanism underlying the Maf-mediated inhibition of *Pparg* expression and adipogenesis, we examined the effect of Maf on the transcriptional activity of Cebp, the family members of which are involved in the regulation of *Pparg* (27, 28). Overexpression of Maf clearly suppressed the activation of the *Pparg* promoter by Cebpα and Cebpδ but not that by Cebpβ (Figure 4E and data not shown). Since the introduction of mutation(s) into MAREs in the *Pparg* promoter did not affect the inhibitory effect of Maf on Cebpδ activity, it is unlikely that Maf inhibited the *Pparg* promoter activity by directly binding to MAREs (Supplemental Figure 16, A and B). EMSA revealed that Maf did not affect the

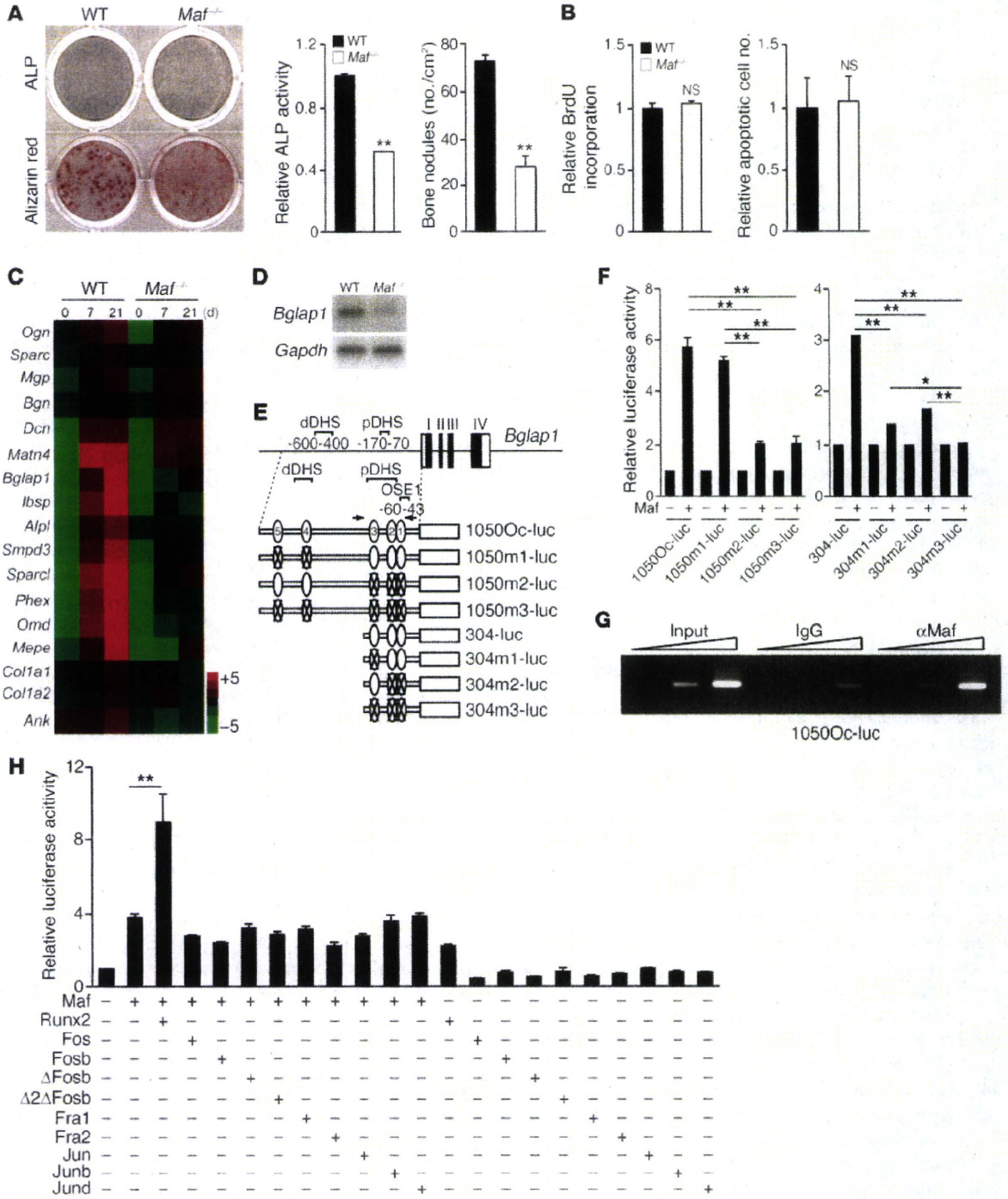

Figure 2

Regulation of osteoblast differentiation and *Bglap1* expression by Maf in cooperation with Runx2. (**A**) ALP and alizarin red staining of WT and *Maf*$^{-/-}$ calvarial cells. ALP activity and bone nodule formation were quantitated. (**B**) Proliferation and apoptosis of WT and *Maf*$^{-/-}$ calvarial cells. (**C**) mRNA expression of osteoblast-specific genes in WT and *Maf*$^{-/-}$ calvarial cells (GeneChip analysis). (**D**) *Bglap1* expression in WT and *Maf*$^{-/-}$ calvarial cells cultured with osteogenic medium for 7 days (RNA blot analysis). (**E**) Schematic of 5 MARE-like sequences (MARE1–MARE5) in the regulatory region of *Bglap1*, and *Bglap1*-luc variants harboring point mutation(s) in MARE-like sequences. pDHS and dDHS indicate proximal and distal DNase hypersensitive sites, respectively (23). Arrows indicate the primer set used for ChIP. Numbers within ovals represent corresponding MARE sequences. Ovals with "X"s indicate sequences without that respective MARE sequence. (**F**) Effect of Maf on the *Bglap1*-luc variants. (**G**) Recruitment of Maf to the *Bglap1* promoter region containing MARE1–MARE3. Calvarial cells cultured with osteogenic medium for 7 days were analyzed by ChIP. (**H**) Effect of Runx2 and AP-1 family members on Maf-mediated activation of 1050Oc-luc. $^{*}P < 0.05$; $^{**}P < 0.01$.

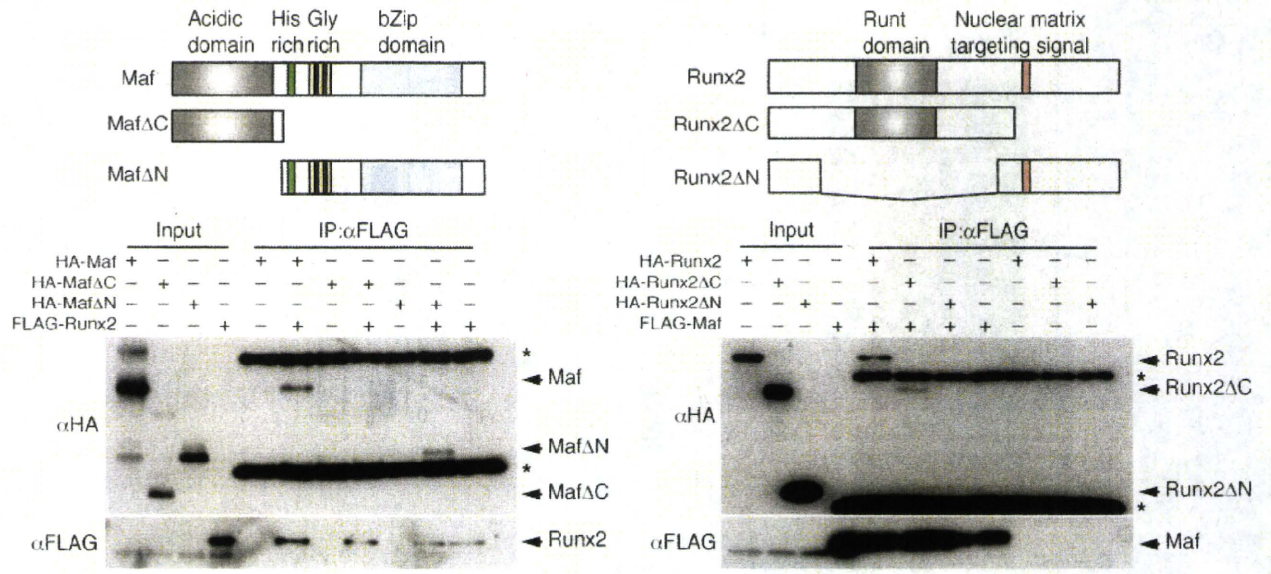

Figure 3

Physical interaction of Maf with Runx2. Maf and MafΔN, but not MafΔC, bound to Runx2. Runx2 and Runx2ΔC, but not Runx2ΔN, bound to Maf. Maf contains a transactivated domain (acidic domain), a histidine cluster (His rich), glycine stretches (Gly rich), and a basic leucine zipper domain (bZip domain). The asterisk indicates nonspecific bands.

DNA binding activity of Cebpδ, further supporting Maf-mediated inhibition of the *Pparg* promoter being independent of Maf binding to DNA (Supplemental Figure 16C). In addition, AP-1 family members and Runx2 did not affect Maf-mediated inhibition of the *Pparg* promoter (Supplemental Figure 16D). As it has been documented that Maf and Cebpδ commonly use CREB-binding protein gene (Crebbp) as their crucial transcriptional coactivator (29) (Supplemental Figure 8), we inferred that competition for the limited amount of Crebbp accounts for the inhibitory effect of Maf on the Cebpδ activity. As expected, the interaction of Cebpδ with Crebbp was suppressed by the overexpression of Maf (Figure 4F). Overexpression of Crebbp recovers the Maf-mediated inhibition of the effect of Cebpδ on the *Pparg* promoter (Figure 4E), lending support to the notion that Maf inhibits Cebpδ activity due to Crebbp squelching, although this may not be the sole mechanism underlying Maf inhibition of adipogenesis.

Decreased Maf expression accelerates age-related osteoporosis and fatty bone marrow. Although the perinatal lethality of *Maf*$^{-/-}$ mice renders it difficult to evaluate the development of fatty marrow with aging, the expression of *Pparg* in the bone marrow is much higher in perinatal *Maf*$^{-/-}$ mice than WT mice (Figure 5A), suggesting that the adipogenesis is enhanced in vivo in the case of *Maf* deficiency. Haploinsufficiency of *Maf* did not affect bone formation in embryos or neonatal mice (Figure 1B and Supplemental Figure 17). At the age of 22 weeks, however, histological analysis revealed that the bone marrow was filled with adipocytes characterized by fat vacuoles, and the bone volume was reduced in the *Maf*$^{+/-}$ mice (Figure 5, B and C, and Table 2). In contrast, no abnormalities in cartilage were found in the adult or neonatal *Maf*$^{+/-}$ mice (Supplemental Figures 6 and 18). The accelerated fatty marrow formation was accompanied by a decrease in osteoblast number and bone formation (Figure 5D), while osteoclastic bone resorption was not affected in the *Maf*$^{+/-}$ mice, with the serum calcium and phosphate levels being normally maintained (Supplemental Figures 19–21). Thus, haploinsufficiency of *Maf* results in enhanced adipogenesis and decreased osteogenesis in vivo, which was obvious at an advanced age, suggesting that the decreasing level of *Maf* with age contributes to the age-related switch in mesenchymal cell differentiation into adipocytes rather than osteoblasts.

To determine whether forced expression of Maf in mesenchymal cells would rescue an aging phenotype of *Maf*$^{+/-}$ mice, we overexpressed Maf in calvarial cells by retroviral transfer and transplanted them into the femurs of aged mice (Supplemental Figure 22). *Maf*$^{+/-}$ mice transplanted with Maf-transduced calvarial cells had a higher trabecular bone mass (but not cortical bone mass) and a decreased number of intramedullary adipocytes compared with those transplanted with mock-infected calvarial cells (Figure 6A and Table 3). We observed similar results when we transplanted Maf-transduced calvarial cells into aged WT mice (Supplemental Figure 22D). These results indicate that overexpression of Maf resulted in effective restoration of both an accelerated aging phenotype in *Maf*$^{+/-}$ mice and age-related changes in WT mice.

ROS regulation of Maf expression through Trp53. How is *Maf* expression regulated during aging? Since it has been reported that age-related bone loss is related to an increased expression of the Wnt inhibitor secreted frizzled-related protein 4 (30) or a decreased production of soluble factors, such as IGF1, TGFB1, IL-11, and bone morphogenetic protein 2 (6, 14, 15), we evaluated the effect of these factors as well as the effect of ROS on *Maf* expression. Although none of the soluble factors increased *Maf* expression in osteoblast precursor cells (Supplemental Figure 23), treatment with the hydrogen peroxide led to a marked decrease in *Maf* expression, which was restored by the addition of the antioxidant *N*-acetylcysteine (Figure 6B). These results prompted us to investigate whether administration of *N*-acetylcysteine rescue the bone phenotype of *Maf*$^{+/-}$ mice. As expected, administration of *N*-acetylcysteine led to an increased bone mass and decreased intramedullary fat in *Maf*$^{+/-}$ mice (Figure 6, C and D).